JOURNAL OF CHEMICAL EDUCATION

pubs.acs.org/jchemeduc

Laboratory Experiment

Artificial Neural Networks Applied to Colorimetric Nanosensors: An Undergraduate Experience Tailorable from Gold Nanoparticles Synthesis to Optical Spectroscopy and Machine Learning

Davide Revignas and Vincenzo Amendola*

Cite This: *J. Chem. Educ.* 2022, 99, 2112–2120

Read Online

ACCESS | Metrics & More | Article Recommendations | Supporting Information

ABSTRACT: Nowadays, technologies involving nanoparticles, colloids, sensors, and artificial intelligence are widespread in society, media, and industry. It is thus mandatory to integrate them into the curricula of students enrolled in chemistry and materials science. To this purpose, we designed a simple assay for the detection of glutathione (GSH) using surface-clean gold nanoparticles (Au NPs). The alteration of the electric double layer of the Au NPs with increasing GSH concentration causes the particles to aggregate, producing a measurable change in color. This behavior, which is widely exploited for optical sensing, has been introduced in an undergraduate course to familiarize the students with the concepts of nanoparticles, colloids, colloidal stability, and sensor features (selectivity, sensitivity, detection range). Nonetheless, there are no analytical models to quantitatively relate the absorption of Au NP colorimetric sensors to analyte concentration, which is the ideal condition for resorting to machine learning (ML). Hence, an artificial neural network was instructed in a students' collective data-sharing experiment about machine learning. Overall, the laboratory experience is safe and highly tailorable to students' background, course duration, available instruments, and teacher's didactic objectives. For instance, it can be lifted to the Master's or Ph.D. level by improving the spectroscopic and ML contents or shifted toward the industrial ground by focusing on the nanoparticle synthesis. We propose the integration of this laboratory experience in the undergraduate and Master's academic programs to stimulate the students with a collection of hot topics that at the same time can consolidate their preparation on arguments of great relevance for their professional life.

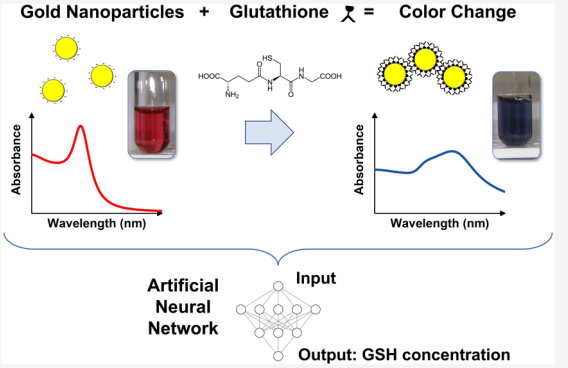

KEYWORDS: *Second-Year Undergraduate, Upper-Division Undergraduate, Physical Chemistry, Computer-Based Learning, Hands-On Learning/Manipulatives, Calibration, Colloids, Nanotechnology, Quantitative Analysis, Spectroscopy*

BACKGROUND

In today's academy, one of the main challenges of teaching is how to cope with the increasing complexity of the contemporary era, embodied by the interpenetration of multiple disciplines and technologies at all levels. It is thus mandatory to find new sustainable and effective ways to convey diverse concepts, starting with the first years of teaching, to endow students with the required set of skills and competencies asked to the modern workforce. In effect, students are aware of the global run to new complex technologies even when these are not yet found in academic syllabi, as demonstrated by their demand for hot scientific and technological topics.

In chemistry and materials science, there is no doubt that nanoparticles, colloids, sensors, and artificial intelligence (mostly machine learning) are examples of such ubiquitous and rapidly expanding fields.[1,2] Industry's increasing interest makes mandatory their inclusion in academic courses, at least with a basic introduction to expose students to the jargon and technical pillars of apparently disparate disciplines. It is also important to show that such new technologies can be integrated and, in the near future, successfully used in both laboratories and workplaces.

With this aim, we organized a lab experience for the colorimetric detection of a peptide, glutathione (GSH), based on the evolution of the optical properties of colloidal gold nanoparticles (Au NPs) when their electric double layer is altered by the analyte, causing particle aggregation. This nanosensor is prepared and calibrated in the lab, and subsequently, the data (absorption spectra) are analyzed

Received: December 30, 2021
Revised: March 21, 2022
Published: April 15, 2022

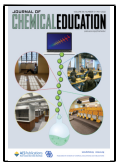

https://doi.org/10.1021/acs.jchemed.1c01288
J. Chem. Educ. 2022, 99, 2112–2120

both empirically and with the support of machine learning by the instruction of an artificial neural network in a students' collective data-sharing endeavor.

Nanosensors with Gold Nanoparticles

Nanomaterials are well-established technologies that are exploited by industry in diverse sectors, ranging from the mechanical properties of nanocomposites to catalysis and biomedicine. A remarkable example is the development of modern biosensors,[3,4] a field where Au NPs have occupied quite a unique position since their introduction in lateral flow immunoassays, such as the pregnancy or antigenic COVID tests available on the home's shelf. In effect, the properties of Au NPs make them an ideal choice for optical nanosensors in which analyte concentration is transduced into a change of color and absorption spectrum.[3,5] Colloids of isolated spherical Au NPs are intensely colored even at particle concentrations as low as 10^{-9} to 10^{-8} M (Au atom concentration of 10^{-4} M) because of the absorption generated by the collective excitations of conduction electrons (called plasmons). This band is located near 520 nm for Au nanospheres with a radius of 10−20 nm, conferring the typical bright-red color recognized for centuries (Figure 1A).[5] The plasmon band is

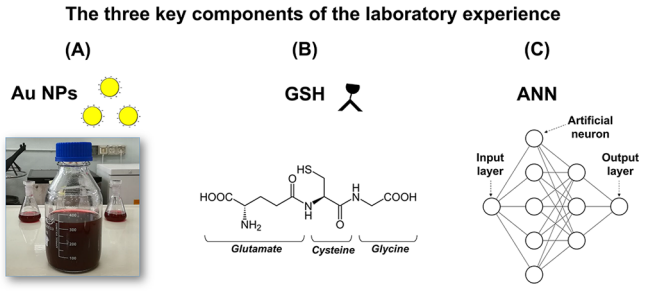

Figure 1. Sketch of the three key components of the laboratory experience: (A) Au NPs, (B) GSH, and (C) an ANN.

sensitive to the interparticle spacing, meaning that aggregation of the particles is associated with a remarkable red shift and broadening of the absorption peak. This enables the aggregation of the particles to be followed by eye or with a UV−vis spectrophotometer. Thus, it is no surprise that chemically engineered Au NPs have been exploited in a large panel of bioanalytical assays where the surfaces of the Au NPs are coated with analyte-binding functionalities that enable particle aggregation and color change in relation to the analyte concentration.[3] This is easily possible because the gold surface binds strongly to thiol functional groups through covalent bonding, enabling conjugation with chemical components selective for each desired analyte.

Besides, Au NPs are thermally stable and photostable, chemically inert, and biocompatible, and colloids of monodisperse Au NPs can be prepared by simple wet-chemical methods[6] or by laser ablation in liquid[7] without the need for expensive or sophisticated equipment.

Such a range of positive features has not gone unnoticed in this *Journal*, which has published several contributions on integration of the synthesis, properties, and sensing applications of Au NPs into graduate and undergraduate university syllabi.[6,8,9] Nonetheless, to the best of our knowledge, our practical experience is the first one to connect machine learning with the use of Au NPs as colorimetric sensors for a peptide.

Glutathione

The important role of nanotechnology in the bioanalytical field and the consequent need for students to gain basic knowledge on the use of nanotechnology products for practical applications suggested the creation of a colorimetric assay for a biomolecule like GSH. This was inspired by previous reports in the scientific literature about the detection of thiol-containing amino acids such as homocysteine and cysteine or GSH using gold nanoparticles.[10,11]

GSH is the nontoxic tripeptide γ-glutamyl-cysteinyl-glycine (Figure 1B) that is ubiquitous in eukaryotic cells, where it is the most abundant non-protein thiol.[10,11] GSH plays an important antioxidant and detoxification role. For instance, GSH is necessary for removal of harmful organic peroxides and free radicals and can also bind to several toxic metals, solvents, and pesticides, permitting their excretion.

The peptide bond between the amine group of cysteine and the carboxylic group of the glutamic acid side chain leaves free a thiol group, which can chemically interact with the Au NP surface, and two carboxylic groups, which can form hydrogen bonds at nonbasic pH with a second GSH molecule bound to another Au NP.[10,11] Overall, the binding of GSH to the surfaces of Au NPs, based on the high affinity of thiolated species for gold surfaces, will promote particle aggregation and color change. These effects grow with the progressive formation of a layer of peptides on the available Au NP surfaces. Thus, the unique optical properties of Au NPs and their binding affinity with GSH provide an excellent opportunity to address in a single practical session several fundamental aspects related to sensors, colloid stability, interactions of nanoparticles with biomolecules, and data analysis.

However, no analytical models exist to quantitatively relate the optical absorption of Au NPs aggregated in the presence of the analyte to the analyte concentration itself, which is the ideal case for resorting to machine learning.

Machine Learning with Artificial Neural Networks

Artificial intelligence (AI) has rapidly grown from science fiction to everyday life, where it has a fundamental role in several sectors such as web chats, self-driving cars, face-recognition functions in smartphones, and translation of written text and speeches as well as many other less apparent but equally pervasive aspects such as medical imaging, spam filters, online recommendations, and fraud detection.[12] In the field of AI, machine learning (ML) is a major group of informatic methods that enable machines to autonomously learn from data in order to identify patterns and correlations of technical utility.[13]

Frequently, ML is operated by resorting to artificial neural networks (ANNs), which are sets of interconnected computing elements called artificial neurons by analogy to the supposed models of how biological neurons work in living organisms (Box 1).[14] In effect, the function of an ANN is to analyze a large input set of correlated data to identify a corresponding set of weights that best describe the correlations in the dataset. This is especially useful when the dataset is extremely large and the recognition of a pattern or a correlation is not trivial, not apparent, or even not understood. The performance of an ANN increases with the size of the dataset and optimization of the structure of the neural network. Artificial neurons are organized in "layers" placed between the input and the output (see Figure 1C). Each layer is composed of a variable number

https://doi.org/10.1021/acs.jchemed.1c01288
J. Chem. Educ. 2022, 99, 2112−2120

Box 1. ML Jargon

Artificial neural network: a collection of interconnected computing elements (***nodes*** or ***neurons***) organized in layers.

Layer: a group of nodes. At least three layers exist: an ***input layer***, which receives information; an ***output layer***, which returns information; and one or more ***hidden layers***, which process information. A maximum of two hidden layers is needed to model any mathematical function.

Feed-forward ANN: a network in which the information proceeds only from the input to the output layer (when this is not the case, the network is called ***recurrent***).

Supervised training: training approach in which the ANN is provided with a dataset of inputs and the related outputs (in our case, each input absorption spectrum is provided with the corresponding GSH concentration).

Epochs: iterations of the ANNs during the learning process. Epochs stop when the error in the validation set is not reduced anymore.

Training set: a subset of all the available data that is used for the learning process.

Validation set: another subset of the available data that is not used for training but is instead used to evaluate the performance of the ANN over "unknown" data (i.e., its generalization capability) at different epochs of the training process.

Overfitting: the undesired situation in which the ANN reproduces well the training set but not the validation set (i.e., the ANN has a large generalization error).

Early stopping: a training technique used to avoid overfitting in which the training is stopped when the performance of the ANN on the validation set does not improve anymore.

Test set: a subset of all the available data that is distinct from the training and validation sets and can be used to compare the performances of ANNs with different ***hyperparameters*** (i.e., different numbers of layers, different numbers of neurons, etc.)

of neurons, which also depends on the nature of the input and output. Each neuron of the first layer receives the input and transfers it to the neurons of the next layer by applying a weight, whose identification and optimization is the scope of the computational ("learning") process.

The versatility of ANNs has few analogues, if any, suggesting that applications of ANNs will penetrate deeply in all sectors, including chemistry and materials science.[13,14] The advances in computational power and ML algorithms have now brought into academic and industrial practice the analysis and correlation of large amounts of experimental and theoretical data about chemical compounds and materials. As a result, ML is routine for the optimization of catalysts, the description of physical properties of bulk materials, the prediction of interaction potentials, and the identification of synthetic parameters for a specific product.[2] Recognition of absorption spectra, which is implemented in this practical experience, is another frequently sought task for ML.[15] For instance, the first review of the application of ML in chemistry, dated 1991, described the use of neural networks for the analysis of mass, IR, UV−vis, and NMR spectra to infer protein structure.[16] In the field of plasmonics, the number of studies resorting to ML for classification and prediction of optical properties also is rapidly growing.[17−19]

The widespread use of ML urges the familiarization of the next generation of scientists and researchers with this technology. This *Journal* has been contributing to the introduction of ML and ANN concepts and computational experiences since 1994.[14] Nonetheless, a key point for teaching is how ML can be used in the specific context of the experimental practice of chemistry and materials science beyond the theoretical and computational field.[12,13] The laboratory experience proposed here offers the opportunity of molding the next generation of researchers for a future where empirical processes and experimental practice will be systematically supported by self-learning machines.

The Laboratory Experience

The laboratory experiment was designed for a class of ∼60 students of the second year of the B.Sc. in Industrial Chemistry, with a student to demonstrator ratio of 12−16:1. The demonstrator supervised three or four groups of students working in two 4 h sessions dedicated to the experimental part (with one UV−vis spectrometer for every two groups) and data analysis, respectively. For the ML part, the data were processed through an ANN provided within a MATLAB environment. A 2 h introduction to the conceptual background of the experience (sensors, gold nanoparticles, colloid stability, ANNs, and expected data analysis) was provided a few days before the experimental work.

The experience was accomplished by several cohorts of students over the years, but the implementation of the ML part was introduced only in the most recent cohort. In this last case, students' feedback was extremely positive, since the experience received 55% of preferences in an online anonymous pool available on the Moodle page for the course, with the remaining 45% shared among the other experiences of a 64 h laboratory course on physical chemistry (the other five lab experiences were the determination of electrolyte conductivity, spectroscopic estimation of diffusion coefficients of a dye, fluorescence quenching, HOMO−LUMO gap estimation with cyclic voltammetry, and standard potential determination in an electrochemical cell). Students appreciated the instrument-free possibility to monitor the quantity of GSH by the color change, the introduction to the functional and chemical properties of colloidal nanoparticles, the exploitation of ANNs, and the realization of a bioassay they built themselves.

For the students of this laboratory course, it was their first experience in handling, functionalizing, and using nanomaterials, analyzing the data, and writing a detailed laboratory report according to scientific standards. Nonetheless, all groups completed the experimental protocol and the related data analysis. The learning outcomes were assessed by collecting a written report (in electronic format) and evaluated according to the table reported in the Supporting Information (SI).

From a teacher perspective, the laboratory experience has the advantages of being simple, reproducible, safe, and hood-free; being based on inexpensive reagents; requiring ambient conditions; being accomplished with a UV−vis spectrophotometer as the only required instrumentation; and being tailorable to the level of students and intended didactic contents (as discussed also later in this article).

■ EXPERIMENTAL SECTION

Chemicals and Equipment

The experimental procedure involves the following chemicals: Au NPs solution (8 nM in NPs), γ-L-glutamyl-L-cysteinyl-

https://doi.org/10.1021/acs.jchemed.1c01288
J. Chem. Educ. 2022, 99, 2112−2120

glycine (GSH) (≥98.0%, Sigma-Aldrich), and NaOH solution (0.1 M, from NaOH, ≥ 98.5%, Scharlau). All of the chemicals were used as received without further purification. All of the solutions were prepared with double-distilled water (alternatively, Milli-Q water can be used). Au NPs were obtained by laser ablation in liquid (LAL), a green method starting from a 99.99% pure Au plate dipped in a 10^{-4} M NaCl (≥99.5%, Fluka) aqueous solution (see the SI for a scheme of the synthesis setup). The 1064 nm laser pulses (6 ns, 50 Hz, Nd:YAG laser) were focused on the metal plate with an $f = 10$ cm lens at a fluence of 8 J/cm^2. The Au NPs prepared according to this protocol are nearly spherical, with an average size of 16 nm as determined by electron microscopy and fitting of the UV−vis spectrum with the model described in ref 20. Au NPs can be generated at low cost[21] by LAL in any pulsed-laser laboratory following the instructions reported in the *Handbook of Laser Synthesis & Processing of Colloids*[7] or purchased from several companies (a list can be found in ref 21). Besides, an automatic machine for the production of Au NPs with a portable closed-box system has recently been proposed by the company AutoProNANO.[22] Alternatively, Au NPs can be produced by chemical reduction of $HAuCl_4$ with sodium citrate, as described in ref 6.

The laser-generated colloids of Au NPs can be stored in ordinary glass bottles at ambient temperature with a shelf life of several weeks to months, allowing their use for multiple laboratory sessions without changing the experimental results. In any case, UV−vis spectroscopy can be used to confirm the batch quality over time.

In the typical experience, students were provided with a set of glassware and calibrated micropipettes, the stock solutions of Au NPs and NaOH, and a GSH solution with an unknown concentration (to be determined as the scope of their work).

Absorption spectra were collected with an Agilent Cary 60 UV−vis spectrophotometer using disposable plastic cuvettes with a path length of 1.0 cm.

Data analysis was performed with the free software SciDAVis,[23] and ANN calculations were carried out with MATLAB.

Procedure

In the typical experience, the procedure of the first session, which was held in the laboratory, consisted of the following steps (see the SI for details):

- Preparation of a GSH stock solution (10 mg/mL).
- Preparation of 16 standard GSH solutions (from 10 mg/mL to 2 μg/mL by serial dilution) and a reference of distilled water, each with a volume of 3 mL in a glass test tube. The serial dilution is performed with micropipettes, offering an excellent opportunity to train the students in this technique and error propagation theory during data analysis.
- Preparation of the GSH sample with an unknown concentration and its 10-fold dilution, each with a volume of 3 mL in a glass test tube.
- Addition of 1 mL of the Au NP colloid to each of the above test tubes and mixing/shaking to ensure the uniform distribution of the particles.
- Taking pictures of all of the test tubes. The color changes after only a few seconds, permitting the aggregation of Au NPs to be followed in an instrument-free manner. Students were asked to inspect the solutions visually and try to place the two unknown GSH samples in the correct intervals of concentration by comparing their colors to those of the standard solutions. An example of the result that each group should obtain is shown in Figure 2A.

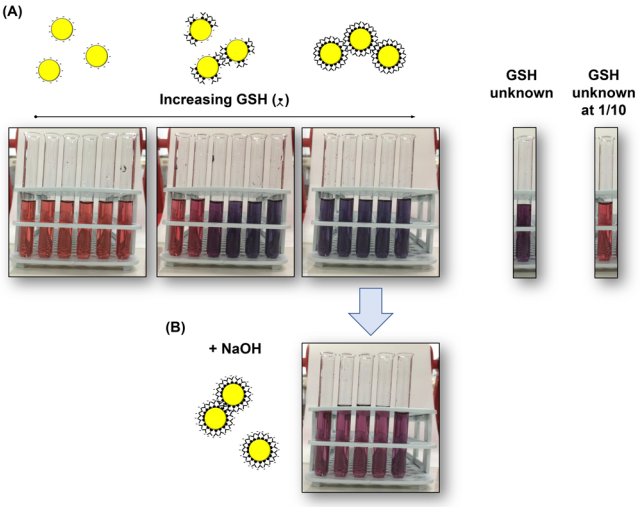

Figure 2. (A) Photographs of the 17 GSH solutions for calibration of the nanosensor and the two solutions with unknown GSH concentration (to be determined in the experience). (B) Effect of addition of NaOH to the solutions with the highest GSH concentration.

- Acquisition of the UV−vis spectra with disposable 1 cm cuvettes. Absorption spectra are typically recorded 10 min after addition of Au NPs to let the system equilibrate but also before precipitation of particles occurs at the highest GSH concentration. It would be optimal to keep a fixed time of preferably 10−15 min between the addition of Au NPs and collection of the UV−vis spectrum for all samples. The registration of UV−vis spectra is normally carried out through cooperation of groups while taking turns at the spectrophotometers. It should be noted that the aggregation state of NPs (and thus the spectrum) may change with time, which can be a large source of error, especially if students are waiting to use spectrometers. Although not tested during the lab experience, a possible strategy to stop or slow down aggregation is the addition of an aqueous solution of the polymer at a fixed time, as described in refs 24 and 25. However, this may be not compatible with the last experimental task after collection of the UV−vis spectra, in which a small volume (ca. 0.5 mL) of 0.1 M NaOH is added to the test tubes with the highest GSH concentration and the disaggregation effect is recorded photographically and by UV−vis spectroscopy. An example is shown in Figure 2B.

It should be noted that the colloidal stability of the Au NPs is sensitive to trace contaminants. Hence, for all of the above operations, the water used must be of the highest purity, and the glassware employed must be scrupulously clean and well-rinsed to avoid uncorrelation of the Au NPs optical properties with GSH concentration.

The procedure for the second session on data analysis consisted of the following steps:

https://doi.org/10.1021/acs.jchemed.1c01288
J. Chem. Educ. 2022, 99, 2112−2120

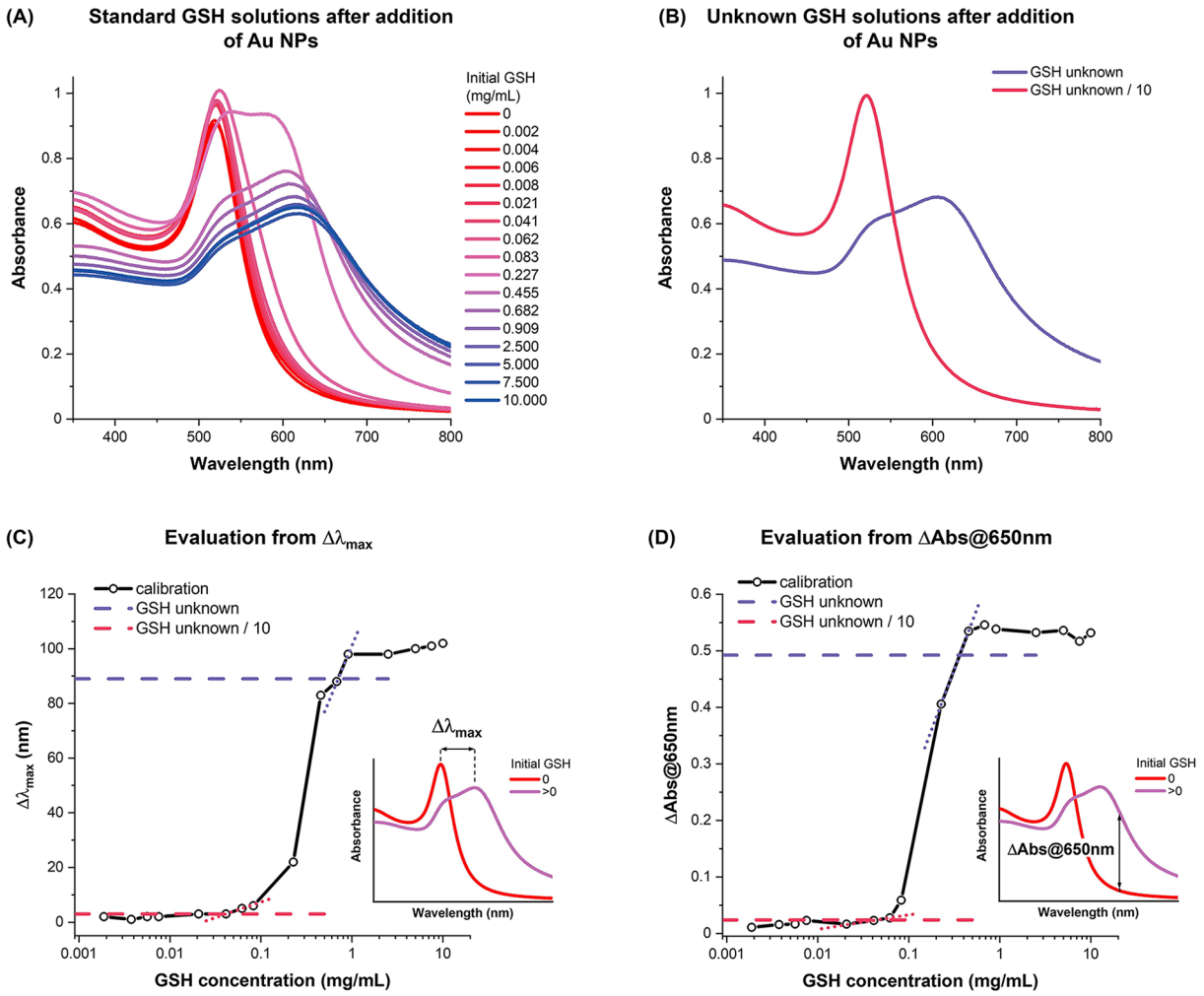

Figure 3. (A, B) UV−vis spectra corresponding to (A) the 17 calibration solutions and (B) the two unknown samples. (C, D) Calibration curves built from changes in (C) the plasmon peak position ($\Delta\lambda_{max}$) and (D) the absorbance at 650 nm (ΔAbs@650 nm). The insets show how the response functions $\Delta\lambda_{max}$ and ΔAbs@650 nm were calculated. The responses of the unknown solutions are represented by the horizontal dashed lines. Dotted lines show the linear interpolations between the pairs of calibration points with response values closest to the values for the unknown solutions.

- Plotting of UV−vis spectra.
- Construction of the empirical calibration curves, with determination of the detection range and sensitivity and evaluation of the GSH concentration in the unknown sample. Each GSH concentration comes with its error.
- Collective experiment for the evaluation of GSH concentration in the unknown sample by instruction of the ANN.

Because of COVID restrictions, data analysis was performed by streaming instead of the standard execution in the computer room of the laboratory. We used the Zoom platform provided by our institution, exploiting the possibility to switch from the main videoconference session for general advice to breakout rooms for individual groups of students (using the breakout room preassign function available on the Zoom home page of the videoconference host) for student- and group-specific advice.

HAZARDS

Hoods are not required because the chemicals employed are not volatile or hazardous, except for the NaOH solution (which is caustic). However, the experience should be performed using standard personal protective equipment (safety glasses, gloves, laboratory coats, and enclosed shoes), and before performing the experiment, students should read the safety data sheets of all chemicals to be used, which should be provided at the workstation of each group.

RESULTS

The typical set of UV−vis spectra for the GSH standard solutions is shown in Figure 3A. The spectra show an evolution of the plasmon absorption band, whose maximum (λ_{max}) progressively red-shifts from 518 nm (GSH absent, nanoparticles not aggregated) to 620 nm (highest GSH concentration, complete aggregation of Au NPs) simultaneously with its remarkable broadening. This corresponds to a progressive solution color change from red to gray, which is well-appreciable when the GSH concentration is above ∼0.08 mg/mL. These spectral features can be exploited to construct a calibration curve that allows the quantitative estimation of the GSH concentrations in the unknown samples, whose spectra are shown in Figure 3B.

https://doi.org/10.1021/acs.jchemed.1c01288
J. Chem. Educ. 2022, 99, 2112−2120

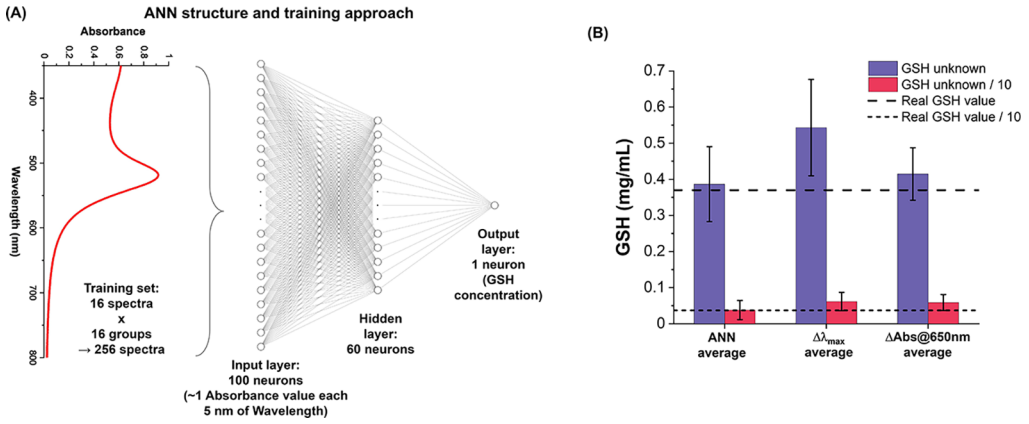

Figure 4. (A) Sketch of the [100|60|1] ANN. (B) Average estimates of the unknown concentrations of GSH solutions with the ANN and the empirical methods. The real values are reported by the dashed and dotted lines.

Empirical Calibration

In the absence of a quantitative model, the simplest way to build a calibration curve is to measure the shift of the wavelength at the maximum of the surface plasmon band ($\Delta\lambda_{max}$) for the different GSH concentrations,[3,5] as shown in Figure 3C. The x scale was converted into the decimal logarithm of GSH concentration to permit a clear visualization of the data points over the 3 orders of magnitude explored during the experiment. Another practical calibration curve consists of reporting the change in absorbance for each solution in the red spectral region (650 nm is suggested, ΔAbs@650nm) versus GSH concentration, as shown in Figure 3D. These empirical curves were useful to introduce the students to the concept of sensors as transducers of a stimulus (GSH concentration) into a well-detectable response (peak shift or absorption increase). These and the other concepts about linear interpolation and calibration were provided to students in the introductory lessons about the lab experience and data analysis for the whole 64 h laboratory course mentioned previously.

Then the response for the unknown GSH solutions was added to the calibration plots (horizontal dashed lines in Figure 3C,D), allowing the quantitative estimation of peptide concentration. It is worth noticing that the calibration curves are generally not describable with a single function, despite resembling a sigmoid, because the initial and the final parts are not exactly flat. At low concentrations, for instance, there could be a red shift of $\Delta\lambda_{max}$ due to coating of the Au NPs with GSH before that aggregation starts, which also is an effect that increases with increasing GSH concentration. However, this effect does not interfere with the calibration because the datasets in Figure 3C,D have the same sigmoidal trend versus GSH concentration and provided comparable results over the various groups of students who performed the lab experience in many different years.

A first rough prediction of the GSH concentration in the unknown samples is possible with the pointer of the data analysis software. However, more precise predictions can be made by finding the intersections between the horizontal lines and the linear interpolations between the pairs data points of the calibration curve with response values closest to those for the unknown samples (dotted lines in Figure 3C,D).

The students were asked to compare the values obtained from the two calibrations and the undiluted and 10-fold diluted samples as an indication of the reliability of the measurement and the compatibility of the two calibrations.

Importantly, from the plots in Figure 3C,D it is immediately evident that the responses of the undiluted and diluted GSH samples are in two regions with much different slopes of the calibration curves. This indicates the importance of sensitivity when a sensor is used to detect a stimulus from an unknown sample. This also explains the didactic utility of using a large range of GSH concentrations. Students were also asked to perform the derivative of the calibration curves to extract the sensitivity over the whole concentration range. This last operation is affected by the experimental error at low and high GSH concentrations, which can be solved by identifying the three main concentration ranges of the calibration curves and making the linear interpolation for each of them (as described in the SI).

Because of the shape of the calibration curves and the wide range of GSH concentrations used, the performance assessment of the nanosensor can be extended to the identification of the lowest and highest detectable quantities, allowing students to become familiar with concepts like the limit of detection (LOD) and maximum detectable limit (MDL).

Calibration with the ANN

At the beginning of the data analysis session, students are introduced to the concept of ML in broad terms, and the basic working principle of ANNs is explained. Afterward, they are asked to share the UV−vis spectra to build a training set large enough for ANNs to be instructed. In the case of our implementation, a total of 256 spectra (16 spectra for 16 groups of students) were collected and exploited to construct the training set (70% of the spectra) and the validation set (all of the remaining spectra) (see the SI for details and comments on the dataset size). This immediately gives the students a demonstration of the utility of ML in the processing of "large" datasets.

An example of a single ANN training can be performed by the demonstrator in front of the student audience, as it takes around 1 min with the optimized parameters that we have selected. The effects of changing the ANN parameters (number of neurons per layer, number of layers, etc.) and advancing training epochs can be also discussed during the demonstration, to show their drastic effects on the predictions and to comment on the concepts of overparametrization and early stopping.

https://doi.org/10.1021/acs.jchemed.1c01288
J. Chem. Educ. 2022, 99, 2112−2120

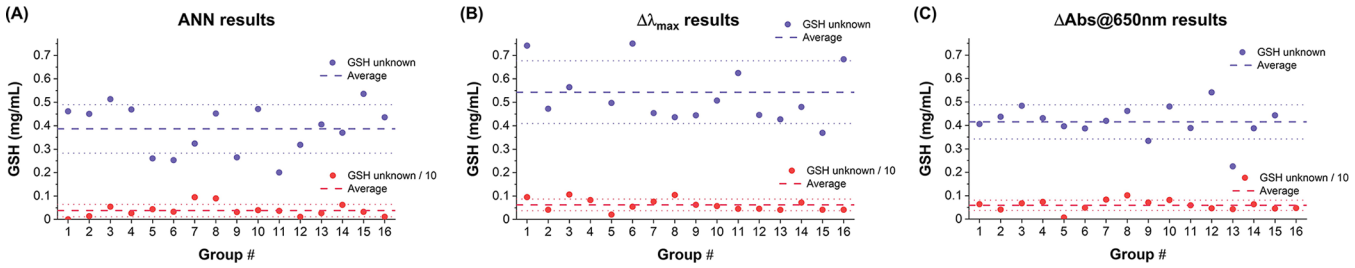

Figure 5. Outputs of (A) the ANN and (B, C) the empirical methods for the unknown solutions of the 16 groups participating in the laboratory experience. Average values and confidence intervals (standard deviation) for the 16 samples are reported as horizontal lines.

To obtain more accurate predictions of the unknown GSH solutions, multiple independent trainings must be performed. With the code provided in the SI, 1 h on a common laptop is typically sufficient, allowing the process to be launched in the background at the beginning of the data analysis session.

We exploited a college-wide MATLAB installation, which has several built-in features specifically suited for ML applications and a relatively friendly graphical user interface. This should overall greatly facilitate students in continuing these activities autonomously in the future.

The structure of the ANN and the type of training were optimized before the demonstration using a dataset collected from the previous cohorts of students. We used a feed-forward network with a layer structure of [100|60|1]. The 100 nodes of the input layer correspond to the absorbances at 100 equally spaced wavelengths in the UV−vis spectra recorded by the spectrometer: this means that the ANN considers all of the spectral information instead of a specific point as in the empirical calibrations. The single node of the output layer corresponds to the GSH concentration for that spectrum. A schematic of the ANN is shown in Figure 4A.

Finally, the ANN can be applied to the spectra of the unknown GSH solutions for each group, to provide an estimation of the concentration. As shown in Figure 4B, the predicted values of the unknown GSH concentration are generally in agreement with the real value (0.370 mg/mL), with a mean value of 0.39 mg/mL and a standard deviation of ±0.10 mg/mL, performing better than the average of the empirical estimations. The observed variability is surely affected by the experimental errors, principally due to dilutions and nonuniform aging time before UV−vis analysis but also to the size of the training dataset (see the SI). For the 10-fold-diluted solution, the mean of 0.038 mg/mL is close to the real value of 0.037 mg/mL but with a standard deviation of ±0.026. However, the lower spectroscopic differences for the diluted GSH sample also affect the empirical evaluation, as is evident from the plots of average (Figure 4B) and single-group concentration estimations (Figure 5).

DISCUSSION

The working principle of the nanosensor relies on the change of colloidal Au NPs from the dispersed state to the aggregated state upon interaction with GSH, which gives rise to new collective-particle surface plasmon absorption at wavelengths longer than 520 nm.[10]

Although colloidal solutions are thermodynamically unstable against phase separation, the Au NPs in this study are negatively charged and repel each other by an electrostatic potential of higher intensity than the attraction potential, as described by the Derjaguin−Landau−Verwey−Overbeek (DLVO) theory.[26] The Au NPs obtained by LAL in NaCl aqueous solutions have a negative charge ascribable to the adsorption of Cl^- ions, as elucidated by recent studies.[27] In Au NPs obtained by chemical reduction, a negative surface charge is also present as a result of adsorption of citrate ions.[10]

The thiol moiety on the cysteine of GSH spontaneously binds to the surface gold atoms of Au NPs within a few seconds, replacing the adsorbed anions. However, the pK_a values for the free carboxylic (2.05 for the glutamate moiety and 3.40 for the glycine moiety) and primary amine (9.49 for the glutamate moiety) groups of GSH are such that they are zwitterionic at neutral pH.[10,11] Thus, the GSH monolayer does not produce an electrostatic double layer like the replaced anions. Besides, several possible interparticle interactions have been suggested to occur in GSH-coated Au NPs, especially intermolecular hydrogen bonding.[10,11] Theoretical calculations identified 12 different intermolecular hydrogen-bonding conformations in neutral GSH, excluding those with the SH group bonded to Au.[11] Hence, the combination of surface charge cleavage and intermolecular interactions upon binding of GSH promotes Au NPs aggregation.

On the other hand, the GSH-mediated assembly of Au NPs should be inhibited at high pH in the solution, as shown after the addition of one drop of NaOH, because of dissociation of the carboxylic groups and restoration of a negative charge on the particle surface. Indeed, the disaggregation lasts for a few minutes before a slow sedimentation process restarts because of the high ionic strength of the solution, corresponding to the shortening of the Debye length in the electrostatic double layer and consequent surface charge shielding.[10]

Finally, we note that the pH of the colloids obtained by LAL is different from that of the colloids obtained by other methods such as chemical reduction with citrate.[28] If the pH of the initial solution changes, also the amounts of GSH and NaOH to be used may be different. For instance, the contribution to aggregation due to hydrogen bonds among carboxylic groups is possible only if the pH is quite low (pH 2−3).

Experience Tailorability

By offering the students an opportunity to familiarize themselves with topics like nanoparticles, bionanomaterial interactions, sensors, colloids, and ML, this experience emphasizes the multidisciplinary approach to modern scientific endeavors. Nonetheless, the structure of the experience could be easily recontextualized according to teaching objectives, course duration, and instrumentation constraints of the laboratory. In Figure 6 we propose a "plug-in" organization of the experience, where each module can be added or removed as desired. Besides, at the level of a really advanced lab course, students may be involved personally in identification of hyperparameters and ANN training.

https://doi.org/10.1021/acs.jchemed.1c01288
J. Chem. Educ. 2022, 99, 2112−2120

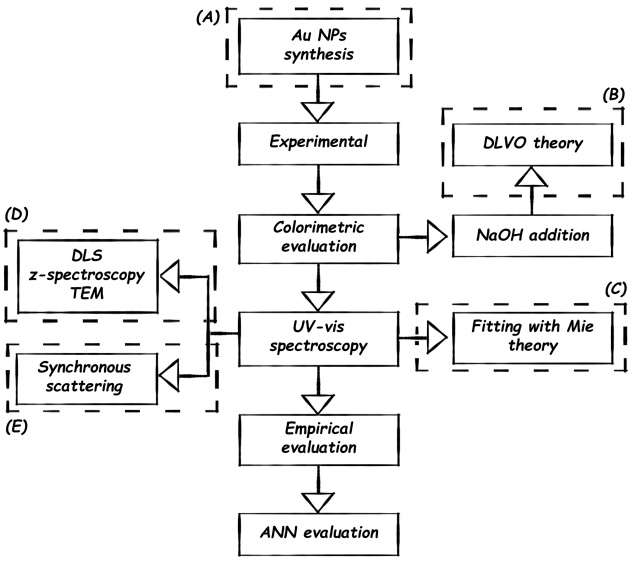

Figure 6. Representation of the laboratory experience as an assembly of "plug-in" modules tailorable to the student type, teacher preferences, and laboratory equipment. Additional modules are highlighted with dashed lines (A–E). For details, see the text.

A first module may consist of the synthesis of Au NPs with LAL or chemical reduction of $HAuCl_4$ (Figure 6A). In our case, the nonspecificity of the Au NPs for the analyte was a deliberate choice to keep the duration of the experience to a single lab session, but a longer time for the practical activity would allow the inclusion of the surface functionalization necessary for a specific recognition ability (e.g., for metal cations).[3,5] The addition of NaOH and the transient disaggregation of GSH-coated Au NPs offers the opportunity to enter into more detail with the DLVO theory (Figure 6B). In our lab experience, students were proposed also to plot a set of interaction potentials representative of Au NP surfaces under the various conditions of the practical experience (see the SI). This part can be also done in a spreadsheet program or with a MATLAB script.

More details on the optical properties of Au NPs can be added, including the Beer–Lambert law or fitting of the absorption spectra with Mie theory (Figure 6C). For instance, a fitting script may be developed by the instructors starting from those described in ref 5, or the Mie and Gans models reported in ref 20 can be used.

Also, the characterization of the colloidal nanoparticles can be expanded with a range of approaches (Figure 6D), from a simple observation of the Tyndall effect to the exploitation of dynamic light scattering (DLS) or z-spectroscopy (a technique for measuring the electrostatic potential at the NP surface) or even transmission electron microscopy (TEM). The characterization of AuNPs can be performed before and after coating with GSH or different compounds and biomolecules. In the case of TEM, it is suggested to use a diluted polymeric matrix to avoid aggregation of the Au NPs during sample deposition, as described in ref 25. Finally, a fluorimeter can also be used in the synchronous scan mode (detection of light elastically scattered from the sample) for an advanced study of the optical properties of aggregated Au NPs (Figure 6E).[5]

On the opposite side, the experience could be adapted to a more general approach by omitting the most advanced aspects.

CONCLUSIONS

We have described a laboratory experience treating several emerging concepts with rapid permeation in modern technologies, such as nanoparticles, colorimetric nanosensors, bionanomaterial interactions, surface functionalization of metal nanoparticles, plasmon absorption, colloids, and data analysis with ML. In addition, basic principles of sensor performance such as calibration, selectivity, sensitivity, and measurement range are directly experienced.

In this practical, the students use a colloid of Au NPs to estimate the quantity of GSH in an unknown solution on the basis of the color change, which is conveniently monitored with UV–vis spectroscopy. Data analysis is performed empirically as well as with collective data sharing to instruct an ANN. The experimental protocol requires safe and affordable reagents and just a UV–vis spectrophotometer, while the ANN part is performed with a standard MATLAB code.

The practical is suitable for students with various scientific backgrounds (chemists, materials scientists, chemical engineers, biologists, biotechnologists, etc.) and levels of study. In effect, the experience is also tailorable to fit the preferred pedagogical objectives, instrument dotation, and lab duration by exploiting the intrinsic "plug-in" modularity of the workflow.

With this experience, the students acquire familiarity with apparently distant concepts like nanotechnology and machine learning, thereby becoming aware of the multidisciplinarity and complexity that will accompany their professional lives.

ASSOCIATED CONTENT

Supporting Information

The Supporting Information is available at https://pubs.acs.org/doi/10.1021/acs.jchemed.1c01288.

Learning outcomes table; scheme of LAL setup for Au NPs synthesis; instructions for students; calculation of sensitivity; DLVO interaction potentials; MATLAB code and procedure; MATLAB code QuickStart guide (PDF, DOCX)

MATLAB code (ZIP)

AUTHOR INFORMATION

Corresponding Author

Vincenzo Amendola − *Department of Chemical Sciences, University of Padova, 35131 Padova, Italy;* orcid.org/0000-0002-9937-7005; Email: vincenzo.amendola@unipd.it

Author

Davide Revignas − *Department of Chemical Sciences, University of Padova, 35131 Padova, Italy*

Complete contact information is available at: https://pubs.acs.org/10.1021/acs.jchemed.1c01288

Notes

The authors declare no competing financial interest.

ACKNOWLEDGMENTS

This research was funded by the University of Padova P-DiSC Project "DYNAMO". D.R. gratefully acknowledges Fondazione CARIPARO for funding his Ph.D. scholarship and "CAPRI:

Calcolo ad Alte Prestazioni per la Ricerca e l'Innovazione" (University of Padova Strategic Research Infrastructure Grant 2017).

REFERENCES

(1) *National Nanotechnology Initiative*. https://www.nano.gov/ (accessed 2021-07-26).
(2) *Computation & Machine Learning for Chemistry*. https://www.nature.com/collections/gcijejjahe/ (accessed 2021-07-26).
(3) Saha, K.; Agasti, S. S.; Kim, C.; Li, X.; Rotello, V. M. Gold Nanoparticles in Chemical and Biological Sensing. *Chem. Rev.* **2012**, *112* (5), 2739−2779.
(4) Huang, C.; Wen, T.; Shi, F. J.; Zeng, X. Y.; Jiao, Y. J. Rapid Detection of IgM Antibodies against the SARS-CoV-2 Virus via Colloidal Gold Nanoparticle-Based Lateral-Flow Assay. *ACS Omega* **2020**, *5* (21), 12550−12556.
(5) Amendola, V.; Pilot, R.; Frasconi, M.; Maragò, O. M.; Iatì, M. A. Surface Plasmon Resonance in Gold Nanoparticles: A Review. *J. Phys.: Condens. Matter* **2017**, *29* (20), 203002.
(6) Roupioz, Y. Functionalization of Gold Nanoparticles for a Color-Based Detection of Adenosine in a Bioassay. *J. Chem. Educ.* **2019**, *96* (5), 1002−1007.
(7) Barcikowski, S.; Amendola, V.; Lau, M.; Marzun, G.; Rehbock, C.; Reichenberger, S.; Zhang, D.; Gökce, B. *Handbook of Laser Synthesis & Processing of Colloids*; DuePublico, 2019. DOI: 10.17185/duepublico/70584.
(8) Njagi, J.; Warner, J.; Andreescu, S. A Bioanalytical Chemistry Experiment for Undergraduate Students: Biosensors Based on Metal Nanoparticles. *J. Chem. Educ.* **2007**, *84* (7), 1180−1182.
(9) Keating, C. D.; Musick, M. D.; Keefe, M. H.; Natan, M. J. Kinetics and Thermodynamics of Au Colloid Monolayer Self-Assembly: Undergraduate Experiments in Surface and Nanomaterials Chemistry. *J. Chem. Educ.* **1999**, *76* (7), 949−955.
(10) Lim, I.-I. S.; Mott, D.; Ip, W.; Njoki, P. N.; Pan, Y.; Zhou, S.; Zhong, C.-J. Interparticle Interactions in Glutathione Mediated Assembly of Gold Nanoparticles. *Langmuir* **2008**, *24* (16), 8857−8863.
(11) Aliakbar Tehrani, Z.; Jamshidi, Z.; Jebeli Javan, M.; Fattahi, A. Interactions of Glutathione Tripeptide with Gold Cluster: Influence of Intramolecular Hydrogen Bond on Complexation Behavior. *J. Phys. Chem. A* **2012**, *116* (17), 4338−4347.
(12) Zawacki-Richter, O.; Marín, V. I.; Bond, M.; Gouverneur, F. Systematic Review of Research on Artificial Intelligence Applications in Higher Education—Where Are the Educators? *Int. J. Educ. Technol. Higher Educ.* **2019**, *16* (1), 39.
(13) Joss, L.; Müller, E. A. Machine Learning for Fluid Property Correlations: Classroom Examples with MATLAB. *J. Chem. Educ.* **2019**, *96* (4), 697−703.
(14) Spining, M. T.; Darsey, J. A.; Sumpter, B. G.; Noid, D. W. Opening Up the Black Box of Artificial Neural Networks. *J. Chem. Educ.* **1994**, *71* (5), 406−411.
(15) Pashkov, D. M.; Guda, A. A.; Kirichkov, M. V.; Guda, S. A.; Martini, A.; Soldatov, S. A.; Soldatov, A. V. Quantitative Analysis of the UV−Vis Spectra for Gold Nanoparticles Powered by Supervised Machine Learning. *J. Phys. Chem. C* **2021**, *125* (16), 8656−8666.
(16) Zupan, J.; Gasteiger, J. Neural Networks: A New Method for Solving Chemical Problems or Just a Passing Phase? *Anal. Chim. Acta* **1991**, *248* (1), 1−30.
(17) Shiratori, K.; Bishop, L. D. C.; Ostovar, B.; Baiyasi, R.; Cai, Y. Y.; Rossky, P. J.; Landes, C. F.; Link, S. Machine-Learned Decision Trees for Predicting Gold Nanorod Sizes from Spectra. *J. Phys. Chem. C* **2021**, *125* (35), 19353−19361.
(18) Hu, J.; Liu, T.; Choo, P.; Wang, S.; Reese, T.; Sample, A. D.; Odom, T. W. Single-Nanoparticle Orientation Sensing by Deep Learning. *ACS Cent. Sci.* **2020**, *6* (12), 2339−2346.
(19) Arzola-Flores, J. A.; González, A. L. Machine Learning for Predicting the Surface Plasmon Resonance of Perfect and Concave Gold Nanocubes. *J. Phys. Chem. C* **2020**, *124* (46), 25447−25454.
(20) Amendola, V.; Meneghetti, M. Size Evaluation of Gold Nanoparticles by UV-Vis Spectroscopy. *J. Phys. Chem. C* **2009**, *113* (11), 4277−4285.
(21) Amendola, V.; Amans, D.; Ishikawa, Y.; Koshizaki, N.; Scirè, S.; Compagnini, G.; Reichenberger, S.; Barcikowski, S. Room-Temperature Laser Synthesis in Liquid of Oxide, Metal-Oxide Core-Shells, and Doped Oxide Nanoparticles. *Chem. - Eur. J.* **2020**, *26*, 9206−9242.
(22) *AutoProNANO*. https://www.autopronano.eu/ (accessed 2021-07-26).
(23) *SciDAVis*. http://scidavis.sourceforge.net/ (accessed 2021-07-26).
(24) Negru, B.; McAnally, M. O.; Mayhew, H. E.; Ueltschi, T. W.; Peng, L.; Sprague-Klein, E. A.; Schatz, G. C.; Van Duyne, R. P. Fabrication of Gold Nanosphere Oligomers for Surface-Enhanced Femtosecond Stimulated Raman Spectroscopy. *J. Phys. Chem. C* **2017**, *121* (48), 27004−27008.
(25) Amendola, V. A General Technique to Investigate the Aggregation of Nanoparticles by Transmission Electron Microscopy. *J. Nanosci. Nanotechnol.* **2015**, *15* (5), 3545−3551.
(26) Israelachvili, J. N. *Intermolecular and Surface Forces*; Academic Press, 2011.
(27) Lévy, A.; De Anda Villa, M.; Laurens, G.; Blanchet, V.; Bozek, J.; Gaudin, J.; Lamour, E.; Macé, S.; Mignon, P.; Milosavljević, A. R.; Nicolas, C.; Patanen, M.; Prigent, C.; Robert, E.; Steydli, S.; Trassinelli, M.; Vernhet, D.; Veteläinen, O.; Amans, D. Surface Chemistry of Gold Nanoparticles Produced by Laser Ablation in Pure and Saline Water. *Langmuir* **2021**, *37* (19), 5783−5794.
(28) Wang, S.; Qian, K.; Bi, X.; Huang, W. Influence of Speciation of Aqueous HAuCl4 on the Synthesis, Structure, and Property of Au Colloids. *J. Phys. Chem. C* **2009**, *113* (16), 6505−6510.

https://doi.org/10.1021/acs.jchemed.1c01288
J. Chem. Educ. 2022, 99, 2112−2120